



Queensland University of Technology
Brisbane Australia

This is the author's version of a work that was submitted/accepted for publication in the following source:

Galpaya, Dilini, Wang, Mingchao, Yan, Cheng, Liu, Meinan, Motta, Nunzio, & Waclawik, Eric R. (2013) Fabrication and characterisation of graphene oxide-epoxy nanocomposite. In *Fourth International Conference on Smart Materials and Nanotechnology in Engineering [Proceedings of SPIE, 8793]*, SPIE - Society of Photo-Optical Instrumentation Engineers , Gold Coast, Qld, pp. 1-7.

This file was downloaded from: <http://eprints.qut.edu.au/61388/>

© Copyright 2013 please consult the authors

Notice: *Changes introduced as a result of publishing processes such as copy-editing and formatting may not be reflected in this document. For a definitive version of this work, please refer to the published source:*

<http://dx.doi.org/10.1117/12.2026759>

Fabrication and Characterisation of Graphene oxide-Epoxy Nanocomposite

Dilini Galpaya¹, Mingchao Wang¹, Cheng Yan^{1*}, Meinan Liu², Nunzio Motta¹, Eric Waclawik¹
¹School of Chemistry, Physics and Mechanical Engineering,
Queensland University of Technology, Brisbane, Australia
²i-Lab, Suzhou Institute of Nano-Tech and Nano-Bionics, Chinese Academy of Science, Suzhou,
China

ABSTRACT

Adequate amount of graphene oxide (GO) was firstly prepared by oxidation of graphite and GO/epoxy nanocomposites were subsequently prepared by typical solution mixing technique. X-ray diffraction (XRD) pattern, X-ray photoelectron (XPS), Raman and Fourier transform infrared (FTIR) spectroscopy indicated the successful preparation of GO. Scanning electron microscopy (SEM) and Transmission electron microscopy (TEM) images of the graphite oxide showed that they consist of a large amount of graphene oxide platelets with a curled morphology containing of a thin wrinkled sheet like structure. AFM image of the exfoliated GO signified that the average thickness of GO sheets is ~1.0 nm which is very similar to GO monolayer. Mechanical properties of as prepared GO/epoxy nanocomposites were investigated. Significant improvements in both Young's modulus and tensile strength were observed for the nanocomposites at very low level of GO loading. The Young's modulus of the nanocomposites containing 0.5 wt% GO was 1.72 GPa, which was 35 % higher than that of the pure epoxy resin (1.28 GPa). The effective reinforcement of the GO based epoxy nanocomposites can be attributed to the good dispersion and the strong interfacial interactions between the GO sheets and the epoxy resin matrices.

Key words: Graphene oxide, epoxy nanocomposites, mechanical properties

1. INTRODUCTION

Since its discovery in 2004¹ graphene, an atomically thick sheet of sp²-hybridized carbon atoms in a hexagonal two-dimensional lattice has attracted a great attention from research community due to its extraordinary physical and electrical properties. The remarkable properties reported for defect free monolayer graphene include high values of its elastic modulus (~1 TPa), intrinsic strength (~130 GPa), thermal conductivity (~5000 W/mK) and specific surface area (2630 m²g⁻¹)^{2, 3}. The superior properties of graphene are reflected in the graphene-incorporated polymer nanocomposites, showing greater mechanical, thermal, electrical, and other properties compared to neat polymer. However, since graphene sheets are inherently stacked in graphite due to the high van der Waals forces between adjacent layers, the exfoliation and incorporation of graphene into polymer matrix to synthesize graphene reinforced polymer is quite difficult. In contrast, graphene oxide (GO) sheets are highly oxygenated and that can alter the van der Waals interactions significantly and be more compatible with organic polymers. This renders GO a good candidate for polymer composites⁴.

Several studies have been conducted to improve mechanical and physical properties of polymeric composites with graphene oxide based materials⁴⁻⁶. Wang et al. reported the incorporation of 0.3% of GO into polybenzimidazole (OPBI) enhanced Young's modulus by 17%, tensile strength by 33% and toughness by 88%. Significant toughness and fatigue life improvements through the addition of GO sheets to a thermosetting epoxy system have been established⁵. Because of oxygen functional groups, graphene oxide can be further functionalized which can effectively increase the reactive points on the GO surface, bring extra advantages to improve the dispersion and interactions of GO in polymer matrices. Several studies have reported significant improvement of polymer with the incorporation of functionalized GO^{7, 8}. One study reported that the less oxidized GO was more effective than nearly fully oxidized GO in terms of reinforcing polymers. The better reinforcement effect was attributed to the higher quality of GO with much fewer

*c2.yan@qut.edu.au; phone +61731386630; fax: +61731381516

structural defects⁹. Zhang et al found that polarity matching is crucial in improving the interaction between fillers and matrix and the dispersion of fillers. They have reported that the excessive oxygen groups on graphene disturbed the polarity matching and deteriorate the dispersion quality of GO in PMMA¹⁰.

However, for the time being, a relatively limited number of studies have been done on enhancing mechanical properties of epoxy through the incorporation of graphene oxide. Herein, we report the tensile and thermal properties of an epoxy matrix reinforced with various weight fractions of graphene oxide. Bulk quantity of graphene oxide was prepared by chemical oxidation method and significant enhancement in tensile properties was achieved by incorporating of small amount of graphene oxide into epoxy matrix.

2. METHOD

Graphite oxide was prepared by oxidizing graphite in a solution of sulphuric acid, phosphoric acid and KMnO_4 for 12 h based on the work of Marcano and co-workers¹¹. Graphite/graphene oxide was characterized by means of XRD, Raman, FTIR, AFM, SEM and TEM techniques. Graphite oxide was dispersed in acetone (1mg/ml) using ultrasonicator at high amplitude for 1 h. Epoxy resin (DGEBA, GY191, CG Composites, Australia) was added into GO dispersion and mixed at room temperature for 30 minutes. Next, acetone was evaporated by heating the mixture on a magnetic stir plate at 40°C for 3 h. The mixture was placed in a vacuum oven for 12 h at 40°C to ensure that all of the acetone has been removed. After allowing the GO-epoxy slurry to cool down to room temperature, hardener (TETA, HY956, CG Composites, Australia) was added and mixed using high speed shear mixer at 2000 rpm for 6 minutes. The resin mixture was degassed in a vacuum oven at room temperature for 30 minutes. Finally, the mixture was poured into silicon molds and then nanocomposite was pre-cured at room temperature for 24 h, followed by post-curing at 95°C for 6 h. Mechanical, thermal and morphological properties were tested to characterize the nanocomposites.

3. RESULTS AND DISCUSSION

3.1. Characterization of graphene oxide

The graphite oxide is highly hydrophilic and is readily dispersible in water and other organic solvent such as DMF, acetone etc. XRD pattern of graphite oxide and bulk graphite shows in Figure 1(a). A characteristic sharp (002) peak of graphite stacking appeared at $2\theta = \sim 26.5^\circ$ with a corresponding interlayer spacing of $\sim 3.4 \text{ \AA}$. After oxidation of graphite to graphite oxide, the peak shifted downward to a lower angle at $2\theta = \sim 11.0^\circ$ with a matching spacing of $\sim 8.0 \text{ \AA}$ which is similar to graphite oxide solids reported previously^{12, 13}. The larger interlayer spacing of graphite oxide is due to the large amount of polar groups generated between the layers of graphite during oxidation, in which the oxygen and carbon atoms are covalently bonded, leading to an increase in the graphite's crystal lattice length along axis c. The diffraction peak of graphite did not occur in the diffraction spectrogram of graphite oxide, indicating that the graphite had been completely oxidized. Raman spectra of graphite and graphite oxide are given in Figure 1(b). The bulk graphite shows the two intense bands centered at 1581 cm^{-1} (G band) and 2720 cm^{-1} (2D band). The G band is the response of the in-plane stretching motion of symmetric sp^2 C-C bond. The 2D band is the second order of the D band. A very tiny D band was observed for bulk graphite. This proved the absence of a significant amount of defects in the graphite. In contrast, the Raman spectrum of the graphite oxide displays an intense D band centred at 1357 cm^{-1} and a G band at 1607 cm^{-1} . The D band arises from the disruption of the symmetrical hexagonal graphitic lattice as a result of internal structural defects, edge defects, and dangling bonds created by the attachment of hydroxyl and epoxide groups on the carbon¹⁴. D band intensity is directly proportional to the level of defects in the sample and can also be used as a gauge of degree of functionalization when graphene is chemically modified¹⁵. Chemical and structural changes of graphite upon oxidation were detected from FTIR spectrum of graphite oxide (Figure 1(c)). A broad band at $3000\text{-}3700 \text{ cm}^{-1}$ appears in the IR spectrum, which signifies stretching vibration of surface hydroxyls (~ 3400) and water absorption ($\sim 3200 \text{ cm}^{-1}$). The peaks are located at $\sim 1720 \text{ cm}^{-1}$ (C=O stretching) from carbonyl and carboxylic groups, at $\sim 1200 \text{ cm}^{-1}$ (C-OH stretching) from carboxylic groups and at $\sim 1050 \text{ cm}^{-1}$ (skeletal C-O or C-C stretching) peak from carbonyl, carboxylic and epoxy groups, which confirms the presence of oxygen-containing functional groups^{16, 17}. The peak at 1620 cm^{-1} can be assigned to the vibrations of the adsorbed water molecules and also the contributions from the skeletal vibrations of un-oxidized graphitic domains¹⁸.

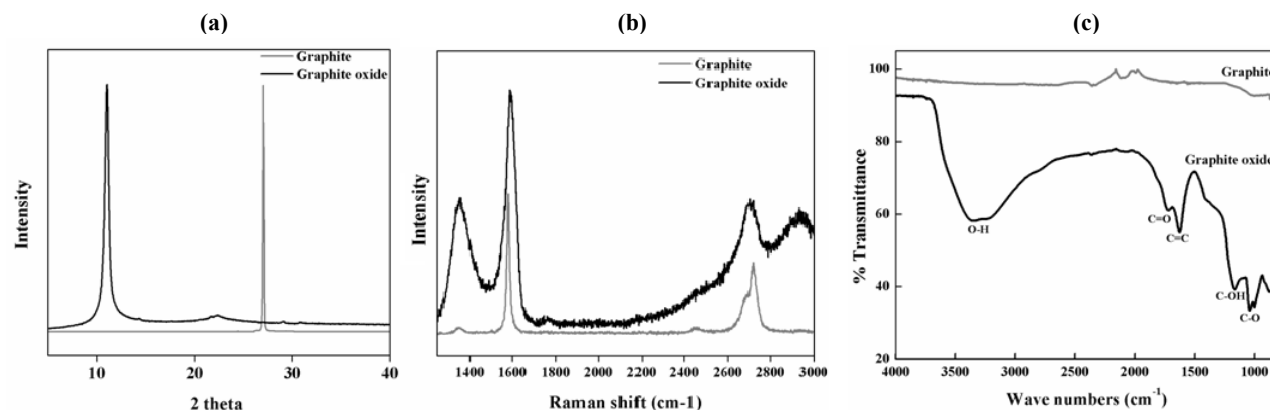


Figure 1. (a) XRD pattern; (b) Raman spectrum; (c) FTIR spectrum of graphite and graphite oxide

The C1s and O1s XPS spectra of graphene oxide were analysed using the CASA XPS software. The data is listed in Table 1. The C1s XPS data of GO surface clearly displays the presence of different kinds of carbon atoms such as non-oxygenated carbons (C-C) at 284.5 eV, carbons in carbon-hydroxyl groups (C-OH) and carbons in epoxy/ether (C-O) at 286.1 eV, and carboxylate carbons (O-C=O) at 288.5 eV. The peaks are at 531.2 eV and 532.9 eV in the O1s data of graphene oxide can be assigned to contribution from C=O/O=C-OH and C-OH groups, respectively¹⁴. Based on the XPS data, calculated oxygen content in graphene oxide is approximately 35%. The chemical composition detected for the graphene oxide is very similar to reported data in literature^{14, 19-21}.

Table 1. Summary of the XPS data analysis for C 1s and O 1s spectra of graphene oxide

Peaks	Binding energy (eV)	(%)
Carbon 1s (1) C-C	284.5	29.1
Carbon 1s (2) C-O-C, C-OH	286.1	23.2
Carbon 1s (3) O=C-OH	288.5	11.5
Oxygen 1s (1) R-CO-R	531.2	11.1
Oxygen 1s (2) C-O-C, C-OH	532.9	23.3

Figure 2(a) illustrates the typical SEM image of graphite oxide, indicating that graphite oxide consists of randomly aggregated, thin crumpled sheets closely associated with each other which are significantly different from graphite flakes. The platelets have lateral dimensions ranging from several hundred nanometers to several micrometers. The TEM observations further reveal that the graphene oxide are likely to be in the form of single or few layer sheets as shown in Figure 2(b). From a tapping mode AFM image of graphene oxide on a mica substrate (Figure 2c), the average thickness is ~ 1 nm. This value is very similar to the reported thickness of graphene oxide monolayer²²⁻²⁴. Compared with the pristine graphene with a thickness of ~ 0.8 nm¹, the higher thickness of as-made GO is due to the presence of the covalent C-O bonds at both top and bottom surfaces, distorted sp³ carbon lattices and absorbed contaminations²⁵⁻²⁷. All these observations indicate that graphite was completely oxidized and exfoliated to GO sheets upon oxidation and sonication.

3.2. Characterization of graphene oxide/epoxy nanocomposites

Tensile test was performed according to the ASTM D638-10 standard with Instron tensile machine using dog-bone shaped tensile specimens. The tests were performed at constant loading speed of 0.5 mm/min with the 2 kN load cell at room temperature. At least five specimens were tested from each sample. Figure 3(a) shows variation of ultimate tensile strength and Young's modulus of neat epoxy and the nanocomposites with different GO content and Figure 3(b) provides the representative tensile stress-strain curves. From the graph (a), it can be seen that Young's modulus and tensile strength of epoxy matrix increased with GO loading. Young's modulus and tensile strength of neat epoxy are 1.28

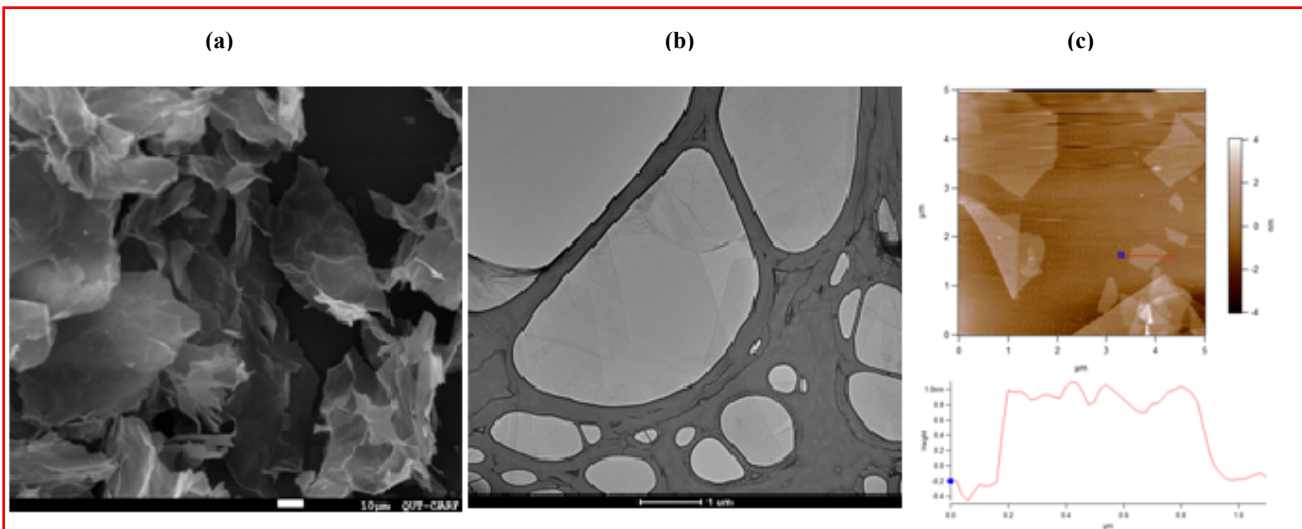


Figure 2. (a) SEM (b) TEM (c) AFM images of graphene oxide

GPa and 49.15 MPa, respectively. The maximum 35% improvement of Young's modulus and 7% improvement of tensile strength were observed the nanocomposite with 0.5 wt% GO. Graph (b) shows that as more GO is incorporated, considerably reduced strains at ultimate strength are observed. The decreased tensile strain of nanocomposites with increasing GO content are typical behaviour of composite with enhanced strength and stiffness²⁸. It is obvious from the results that GO can significantly improve the strength properties of epoxy. Improvement can be credited to high elastic modulus and strength of GO, better interactions between GO and polymer matrix and uniform dispersion of GO in the epoxy matrix due to abundant functional groups on the GO surface²⁹.

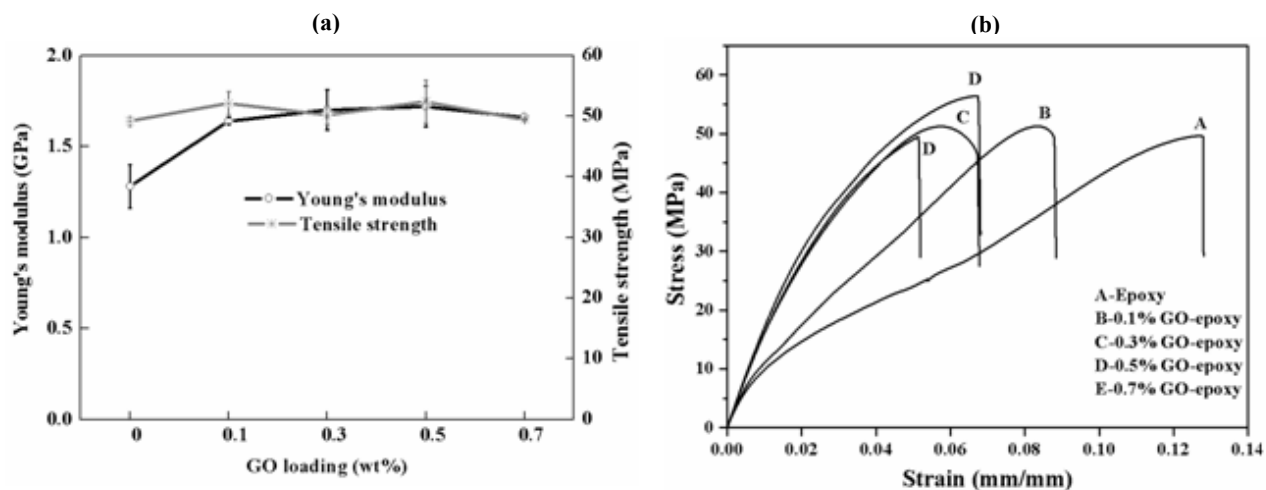


Figure 3. (a) Young's modulus and tensile strength (b) Tensile stress vs tensile strain curves of graphene oxide-epoxy nanocomposites

Glass transition temperature (T_g) of nanocomposites was obtained by differential scanning calorimetry (Q100DSC, Chimaera) at a scanning rate of 5°C/min from -50 to 280°C under nitrogen atmosphere and data is shown in Table 2. T_g of pure epoxy is approximately 66°C. The T_g of baseline epoxy was found to decrease significantly when GO is added to the resin and there was ~15°C decrease in the T_g with the addition of 0.5wt% GO. This suggests that, the GO, when dispersed within the epoxy resin obstructs the curing reaction, resulting in low reaction conversion. This interference may be arisen due to reaction between curing agent (TETA) and the functional groups of graphene oxide. As a result, the

optimized ratio of epoxy and curing agent in curing reaction was impacted. This generally reduces the polymer cross-linkage and increase polymer chain mobility. The less restriction on molecular chain mobility grounds to decrease the T_g ³⁰. However, this result is contrary to the mechanical results which showed the system is stiffer with addition of GO. Therefore, further analysis needs to examine the extend of curing process of epoxy-GO composite using other methods.

Table 2. Glass transition temperature of neat epoxy and nanocomposites

Sample	Glass transition temperature, T_g (°C)
Neat epoxy	66.06
0.1% GO-epoxy	52.02
0.3% GO-epoxy	54.35
0.5% GO-epoxy	51.27
0.7% GO-epoxy	50.96

Cross-section of the tensile fractured surfaces of epoxy and GO/epoxy nanocomposites were examined by SEM in order to observe the distribution of GO in the epoxy matrix (Figure 4). But, no significant difference was observed in images of epoxy and the nanocomposites and it was also not able to observe embedded GO sheets in the epoxy matrix. The reasons for this may be because of very low content of GO in the matrix, 2D sheet structure of GO or similar chemical composition/nature of epoxy matrix and GO. Therefore, other techniques such as high resolution TEM or dynamic modulus mapping techniques need to be utilised to examine the GO dispersion in polymer matrix.

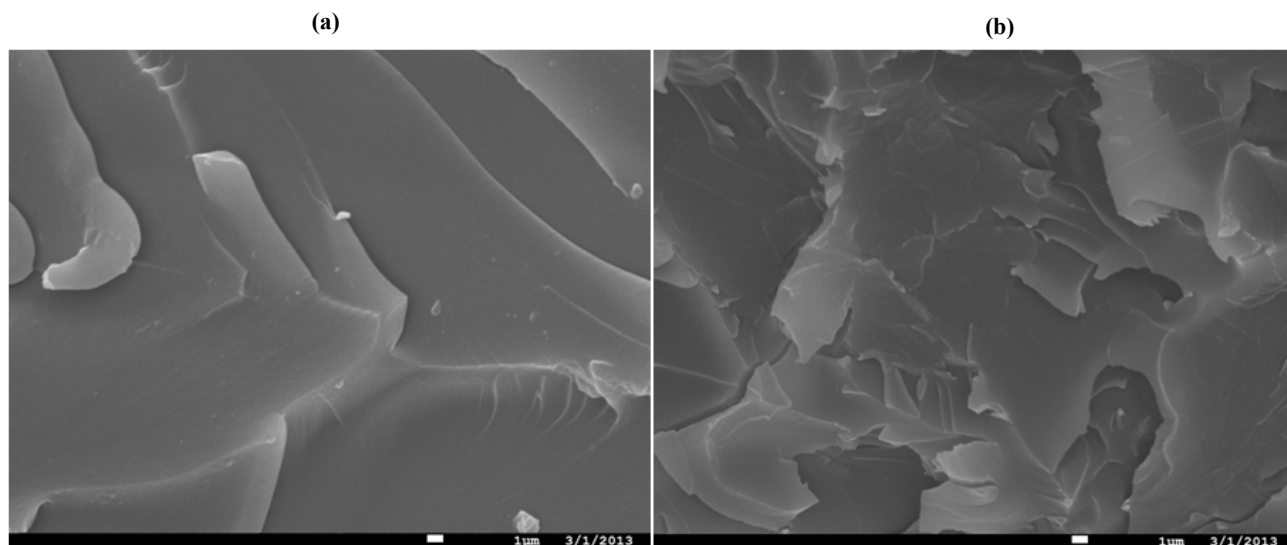


Figure 4. SEM images of tensile fractured surfaces of (a) neat epoxy and (b) 0.7 wt% GO/epoxy nanocomposite

4. CONCLUSIONS

GO with high yield was prepared using a chemical method and produced GO was well dispersed in water and different organic solvents. GO/epoxy nanocomposites were prepared by varying the amount of GO from 0.1 wt% to 0.7 wt%. The maximum 35% improvement of Young's modulus and 7% improvement of tensile strength were observed for the composite with 0.5 wt % loading of GO. However, T_g of baseline epoxy considerably decreased with addition of GO. Further analysis is required to examine curing process and thermal behaviour of composite. SEM technique was not adequate to observe the dispersion of GO sheets in epoxy matrix. Therefore, TEM or dynamic modulus mapping

techniques have to be used for better understanding of GO dispersion and subsequently effect on properties of nanocomposites.

ACKNOWLEDGEMENT

Authors gratefully acknowledge Mr. Marco Notarianni, for his invaluable help for analysis of TEM and XPS data. We would also like to thank University of Queensland and Flinders University, Australia for the facilities provide for TEM and XPS analysis.

REFERENCES

- [1] Novoselov, K. S., Geim, A. K., Morozov, S. V., Jiang, D., Zhang, Y., Dubonos, S. V., Grigorieva, I. V. and Firsov, A. A., "Electric field effect in atomically thin carbon films," *Science*, 306(5696), 666-669 (2004).
- [2] Park, S. and Ruoff, R. S., "Chemical methods for the production of graphenes," *Nat Nano*, 4(4), 217-224 (2009).
- [3] Singh, V., Joung, D., Zhai, L., Das, S., Khondaker, S. I. and Seal, S., "Graphene based materials: Past, present and future," *Prog. Mater. Sci.*, 56(8), 1178-1271 (2011).
- [4] Wang, Y., Shi, Z., Fang, J., Xu, H. and Yin, J., "Graphene oxide/polybenzimidazole composites fabricated by a solvent-exchange method," *Carbon*, 49(4), 1199-1207 (2011).
- [5] Bortz, D. R., Heras, E. G. and Martin-Gullon, I., "Impressive Fatigue Life and Fracture Toughness Improvements in Graphene Oxide/Epoxy Composites," *Macromolecules*, 45(1), 238-245 (2011).
- [6] Kong, J.-Y., Choi, M.-C., Kim, G. Y., Park, J. J., Selvaraj, M., Han, M. and Ha, C.-S., "Preparation and properties of polyimide/graphene oxide nanocomposite films with Mg ion crosslinker," *European Polymer Journal*, 48(8), 1394-1405 (2012).
- [7] Bao, C., Guo, Y., Song, L., Kan, Y., Qian, X. and Hu, Y., "In situ preparation of functionalized graphene oxide/epoxy nanocomposites with effective reinforcements," *Journal of Materials Chemistry*, 21(35), 13290-13298 (2011).
- [8] Cano, M., Khan, U., Sainsbury, T., O'Neill, A., Wang, Z., McGovern, I. T., Maser, W. K., Benito, A. M. and Coleman, J. N., "Improving the mechanical properties of graphene oxide based materials by covalent attachment of polymer chains," *Carbon*, 52(0), 363-371 (2013).
- [9] Wang, Y., Shi, Z., Yu, J., Chen, L., Zhu, J. and Hu, Z., "Tailoring the characteristics of graphite oxide nanosheets for the production of high-performance poly(vinyl alcohol) composites," *Carbon*, 50(15), 5525-5536 (2012).
- [10] Zhang, H.-B., Zheng, W.-G., Yan, Q., Jiang, Z.-G. and Yu, Z.-Z., "The effect of surface chemistry of graphene on rheological and electrical properties of polymethylmethacrylate composites," *Carbon*, 50(14), 5117-5125 (2012).
- [11] Marcano, D. C., Kosynkin, D. V., Berlin, J. M., Sinitskii, A., Sun, Z., Slesarev, A., Alemany, L. B., Lu, W. and Tour, J. M., "Improved Synthesis of Graphene Oxide," *ACS Nano*, 4(8), 4806-4814 (2010).
- [12] Liu, F., Song, S., Xue, D. and Zhang, H., "Folded Structured Graphene Paper for High Performance Electrode Materials," *Advanced Materials*, 24(8), 1089-1094 (2012).
- [13] Compton, O. C., Jain, B., Dikin, D. A., Abouimrane, A., Amine, K. and Nguyen, S. T., "Chemically Active Reduced Graphene Oxide with Tunable C/O Ratios," *ACS Nano*, 5(6), 4380-4391 (2011).
- [14] Yang, D., Velamakanni, A., Bozoklu, G., Park, S., Stoller, M., Piner, R. D., Stankovich, S., Jung, I., Field, D. A., Ventrice Jr, C. A. and Ruoff, R. S., "Chemical analysis of graphene oxide films after heat and chemical treatments by X-ray photoelectron and Micro-Raman spectroscopy," *Carbon*, 47(1), 145-152 (2009).
- [15] Wall, M., "Raman Spectroscopy Optimizes Graphene Characterization " *Advanced Material and Process*, (April 2012).

- [16] Guo, Y., Sun, X., Liu, Y., Wang, W., Qiu, H. and Gao, J., "One pot preparation of reduced graphene oxide (RGO) or Au (Ag) nanoparticle-RGO hybrids using chitosan as a reducing and stabilizing agent and their use in methanol electrooxidation," *Carbon*, 50(7), 2513-2523 (2012).
- [17] Shen, J., Li, T., Long, Y., Shi, M., Li, N. and Ye, M., "One-step solid state preparation of reduced graphene oxide," *Carbon*, 50(6), 2134-2140 (2012).
- [18] Si, Y. and Samulski, E. T., "Synthesis of Water Soluble Graphene," *Nano Letters*, 8(6), 1679-1682 (2008).
- [19] Becerril, H. A., Mao, J., Liu, Z., Stoltenberg, R. M., Bao, Z. and Chen, Y., "Evaluation of Solution-Processed Reduced Graphene Oxide Films as Transparent Conductors," *ACS Nano*, 2(3), 463-470 (2008).
- [20] Fan, X., Peng, W., Li, Y., Li, X., Wang, S., Zhang, G. and Zhang, F., "Deoxygenation of Exfoliated Graphite Oxide under Alkaline Conditions: A Green Route to Graphene Preparation," *Advanced Materials*, 20(23), 4490-4493 (2008).
- [21] Murugan, A. V., Muraliganth, T. and Manthiram, A., "Rapid, Facile Microwave-Solvothermal Synthesis of Graphene Nanosheets and Their Polyaniline Nanocomposites for Energy Storage," *Chemistry of Materials*, 21(21), 5004-5006 (2009).
- [22] Glover, A. J., Adamson, D. H. and Schniepp, H. C., "Charge-Driven Selective Adsorption of Sodium Dodecyl Sulfate on Graphene Oxide Visualized by Atomic Force Microscopy," *The Journal of Physical Chemistry C*, 116(37), 20080-20085 (2012).
- [23] Imperiali, L., Liao, K.-H., Clasen, C., Fransaer, J., Macosko, C. W. and Vermant, J., "Interfacial Rheology and Structure of Tiled Graphene Oxide Sheets," *Langmuir*, 28(21), 7990-8000 (2012).
- [24] Sun, Z., Masa, J., Liu, Z., Schuhmann, W. and Muhler, M., "Highly Concentrated Aqueous Dispersions of Graphene Exfoliated by Sodium Taurodeoxycholate: Dispersion Behavior and Potential Application as a Catalyst Support for the Oxygen-Reduction Reaction," *Chemistry – A European Journal*, 18(22), 6972-6978 (2012).
- [25] Stankovich, S., Dikin, D. A., Piner, R. D., Kohlhaas, K. A., Kleinhammes, A., Jia, Y., Wu, Y., Nguyen, S. T. and Ruoff, R. S., "Synthesis of graphene-based nanosheets via chemical reduction of exfoliated graphite oxide," *Carbon*, 45(7), 1558-1565 (2007).
- [26] Mkhoyan, K. A., Contryman, A. W., Silcox, J., Stewart, D. A., Eda, G., Mattevi, C., Miller, S. and Chhowalla, M., "Atomic and Electronic Structure of Graphene-Oxide," *Nano Letters*, 9(3), 1058-1063 (2009).
- [27] Cheng, M., Yang, R., Zhang, L., Shi, Z., Yang, W., Wang, D., Xie, G., Shi, D. and Zhang, G., "Restoration of graphene from graphene oxide by defect repair," *Carbon*, 50(7), 2581-2587 (2012).
- [28] Lee, J. K., Song, S. and Kim, B., "Functionalized graphene sheets-epoxy based nanocomposite for cryotank composite application," *Polymer Composites*, 33(8), 1263-1273 (2012).
- [29] Du, J. and Cheng, H.-M., "The Fabrication, Properties, and Uses of Graphene/Polymer Composites," *Macromolecular Chemistry and Physics*, 213(10-11), 1060-1077 (2012).
- [30] Jingjing, Q., Chuck, Z., Ben, W. and Richard, L., "Carbon nanotube integrated multifunctional multiscale composites," *Nanotechnology*, 18(27), 275708 (2007).